ChemComm

COMMUNICATION

View Article Online
View Journal | View Issue

Cite this: *Chem. Commun.*, 2023, **59**, 5253

Received 23rd February 2023,
Accepted 3rd April 2023

DOI: 10.1039/d3cc00866e

rsc.li/chemcomm

Coaxial assembly of helical aromatic foldamers by metal coordination†

Albano Galan,[a] Kristijan Lulic,[b] Jingqi Wang,[b] Barbara Wicher,[d] Ivan Huc,[ac] Jean Duhamel[b] and Victor Maurizot *[a]

Deprotonation of acid-terminated helical aromatic foldamers with a mineral base in chlorinated solvents led to their dimerization through the coordination of a metal cation (Li^+, Na^+, K^+, Ag^+, or Hg^{2+}) with the terminal carboxylate functions. This new ligation method was applied to oligomerize diacid-functionalized foldamers.

Foldamers are artificial oligomers that fold into compact molecular architectures inspired by the secondary structures of biomolecules.[1,2] Among the various oligomers and backbones developed in this field, aromatic oligoamides foldamers give access to predictable and robust folded helical conformations with potential applications for protein recognition, as molecular capsules or sensors, or in material science.[3–8] Foldamers have also been used as rigid building blocks for the elaboration of more sophisticated self-assembled structures comprised of multiple independent helices.[9,10] Among these, an interesting architecture is the piling up of helices into rigid coaxial stacks.[11] Such stacks have been promoted in the solid state for example by means of terminal hydrogen-bonding groups[12,13] or metal coordination[14] as well as in solution,[15–18] where they may lead to the formation of fibers.[19,20] Here, we introduce a new, simple and robust end-to-end ligation of helical foldamers based on metal coordination in organic solvent to generate well-defined discrete assemblies and supramolecular metallopolymers.

The starting point of this report is a serendipitous finding made during the solution phase step-wise synthesis of 8-amino-2-quinolinecarboxylic acid helical oligoamides (Fig. 1).[21] Thus, the incomplete protonation of the carboxylate obtained by saponification of a methyl ester led to the observation of two sets of signals in ^{1}H NMR spectra that were assigned to the sodium carboxylate salt and to the expected acid, respectively. Coordination of metal ions by carboxylates is well known.[22–24] Yet, the significant chemical shift differences between the carboxylate and the acid signals and the slow exchange kinetics between the two states on the NMR time scale led us to speculate that the alkaline metal promoted the assembly of oligomers by coordination of their carboxylate end groups.

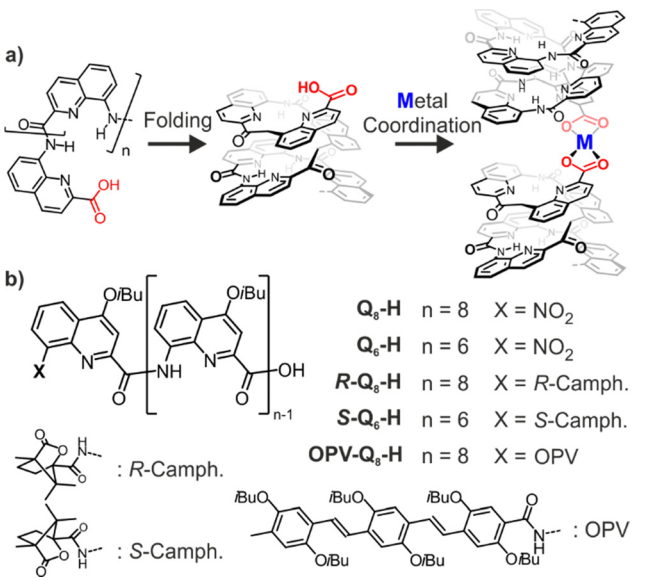

Fig. 1 (a) Schematic representation of the folding of a helical oligoamide quinoline-based foldamer and of the formation of a dimeric complex by metal coordination. (b) Chemical formula of studied compounds.

[a] *Université de Bordeaux, CNRS, Bordeaux Institut National Polytechnique, CBMN (UMR 5248), Institut Européen de Chimie Biologie, 2 Rue Escarpit, Pessac 33600, France. E-mail: victor.maurizot@u-bordeaux.fr*
[b] *Institute for Polymer Research, Waterloo Institute for Nanotechnology, Department of Chemistry, University of Waterloo, 200 University Avenue West, Waterloo, ON N2L 3G1, Canada. E-mail: jduhamel@uwaterloo.ca*
[c] *Department Pharmazie, Ludwig-Maximilians-Universität München, Butenandtstraße 5–13, Munich D-81377, Germany*
[d] *Department of Chemical Technology of Drugs, Poznan University of Medical Sciences, Grunwaldzka 6, 60-780 Poznan, Poland*

† Electronic supplementary information (ESI) available: General synthetic experimental details, NMR spectra, fluorescence anysotropy and X-ray analysis. CCDC 2194086 (Q_8-Na-Q_8), 2194087 (Q_8-K-Q_8), 2194085 (Q_8-Hg-Q_8). For ESI and crystallographic data in CIF or other electronic format see DOI: **https://doi.org/10.1039/d3cc00866e**

In order to better characterize this new ligation, an acid-functionalized quinoline octamer (Q_8-H, Fig. 1) was synthesized based on a well-established protocol.[21] Different methods were explored to prepare the desired metal complexes with this foldamer. In the presence of an excess of NaOH introduced either as a solid suspension or in an aqueous phase, the complex could be detected in a $CDCl_3$ solution of Q_8-H as evidenced by the analysis of the ^{1}H NMR spectrum. A new set of proton signals gradually appeared at the expense of those of the initial Q_8-H (Fig. S1, ESI†) which, according to diffusion-ordered spectroscopy (DOSY) NMR spectra (Fig. S7, ESI†), correspond to a bigger entity than the initial monomeric species. The new signals appeared at lower chemical shifts compared to the initial signals, indicating a strong shielding effect, in agreement with the formation of a stacked duplex. For example, characteristic NH quinoline amide signals and singlets of protons in position 3 of the quinolines were shifted downfield by around 1 ppm in the complex (Fig. 2a and b) and are in the range of those observed for the quinoline hexadecamer.[25] Notably, only one set of signals is observed for the complex, indicating a completely stereoselective assembly of the helices involved. Indeed, helices from a quinoline octamer have a slow helical inversion rate[25] and the NMR spectra are expected to show different signals for complexes composed of helices of similar or opposite helical handedness (*PP*/*MM vs. PM* for dimers)(Fig. S8, ESI†).

The solid-state structure, obtained by X-ray diffraction analysis of single crystals, confirmed the formation of a Q_8-Na-Q_8 dimer (Fig. 3a and d). The two helically folded quinoline octamers have the same handedness and are connected through their carboxylate end group to one sodium cation in a head-to-head fashion with a perfect coaxial arrangement of the helices. The cation is hexa-coordinated to one carboxylate oxygen atom and the endocyclic nitrogen atoms of the two adjacent quinoline rings of each oligomer. The O–Na bonds are

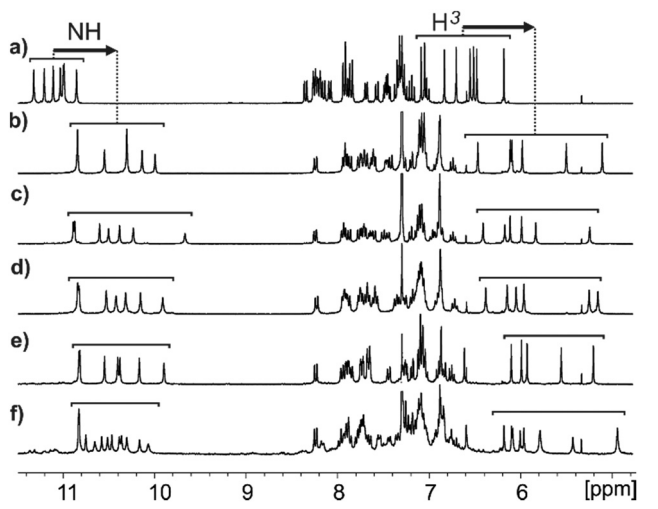

Fig. 2 Downfield region of ^{1}H NMR spectrum of a $CDCl_3$ solution (300 MHz, 298 K, 2 mM) of (a) Q_8-H (b) Q_8-Na-Q_8 (c) Q_8-K-Q_8 (d) Q_8-Li-Q_8 (e) Q_8-Ag-Q_8 (f) Q_8-Hg-Q_8, brackets indicate the amide proton region and proton in position 3 of the quinoline units.

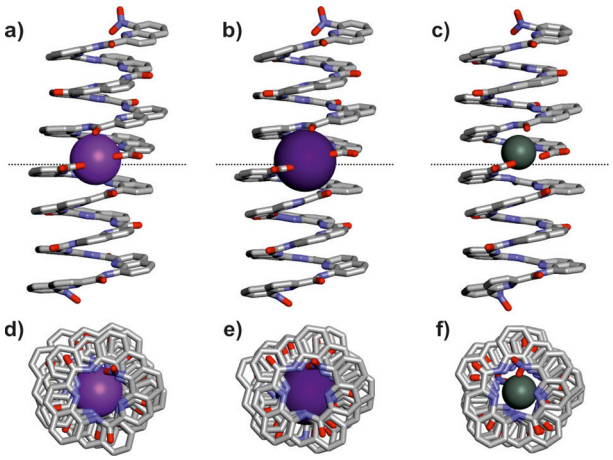

Fig. 3 X-ray structures of dimer complexes. Side view of (a) Q_8-Na-Q_8 (b) Q_8-K-Q_8 (c) Q_8-Hg-Q_8. Top view of (d) Q_8-Na-Q_8 (e) Q_8-K-Q_8 (f) Q_8-Hg-Q_8. Foldamers are shown in sticks, whereas metal cations are displayed as balls. H atoms, side chains, solvent molecules and ions have been removed for clarity. Dashed lines are indicative of the middle of the dimeric structure and do not represent crystallographic symmetry elements.

2.23 and 2.25 Å-long, while the N–Na distances range from 2.69 to 3.05 Å (Fig. S29 and Table S2, ESI†). To fulfill the charge balance, a second sodium cation is located close to the end of the helices but outside the coaxial dimer. It is presumably not involved in the complex stabilization in solution.

The dimerization of Q_8H with NaOH was further studied by time-resolved fluorescence anisotropy (TRFA), which provided a reliable way to evaluate oligomer size and shape. To this end, Q_8H was modified at its N-terminus with a trimeric oligo(phenylene vinylene) to yield the fluorescently labelled OPV-Q_8H (Fig. 1b).[26] Solutions of OPV-Q_8H were prepared in chloroform at concentrations ranging from 13 nM to 830 μM, thus spanning five orders of magnitude. TRFA yielded the average rotational time $\langle\phi\rangle$ of the objects generated in the OPV-Q_8H solutions after adding 0.1 g of 16 M NaOH solution. $\langle\phi\rangle$ was plotted as a function of OPV-Q_8H concentration in Fig. S32 (ESI†). Before exposure to NaOH, $\langle\phi\rangle$ was constant and measured at 0.79 ($\pm$ 0.02) ns for the entire concentration range. This value is similar to the 0.78 ns determined earlier for the methyl ester of OPV-Q_8H.[26] The addition of NaOH led to a sigmoidal increase in $\langle\phi\rangle$ with increasing OPV-Q_8H concentration, going from 0.77 ($\pm$0.01) ns at [OPV-Q_8H] $<$ 46 μM to a constant value of 1.40 ($\pm$0.02) for [OPV-Q_8H] $>$ 100 μM. Since $\langle\phi\rangle$ is directly related to the length of the molecular edifice, its increase indicated the formation of a larger object in solution. Based on an earlier calibration for these methyl ester quinoline oligomers,[26] a 1.40 ns rotational time would be equivalent to a foldamer made of 19 quinolines, slightly larger than the 16 quinolines of an OPV-Q_8-Na-Q_8-OPV dimer. The difference in the expected and actual quinoline numbers (19 *vs.* 16) is presumably due to the second OPV moiety in the dimers since the calibration curve was established with oligomers bearing a single OPV label. Furthermore, the sigmoidal $\langle\phi\rangle$-*vs.*-[OPV-Q_8H] profile in Fig. S33 (ESI†) is a clear indication of a finite (discrete) association mechanism matching the dimerization of OPV-Q_8H rather than non specific association.

The finding that a strong base like NaOH promoted dimerization led to study the effect of less basic salts on dimerization. The Q_8-Na-Q_8 dimer complex was quantitatively produced by treatment of a Q_8-H solution in chloroform with sodium carbonate, although with slower kinetics (Fig. S4, ESI†). The Na^+ dimeric complex was also generated with sodium acetate but not quantitatively, even in presence of a significant excess of the base for a week (Fig. S6, ESI†). The same ^{1}H NMR spectrum was obtained for the complexes regardless of the counteranion used, suggesting that it is absent from (or had little effect on) the dimer structure in the final solution.

Having optimized the preparation of the Na^+ dimer complexes, we then explored whether other metal salts could also produce dimeric complexes. Q_8-H was mixed with various basic salts, and complexation was monitored by ^{1}H NMR. Dimeric complexes were successfully prepared with K^+, Li^+, Ag^+, and Hg^{2+} salts (Fig. 2c–f). Potassium complexes were formed quantitatively when treating Q_8-H with an excess of either potassium hydroxide or carbonate (Fig. 2c and Fig. S9–S11, ESI†). Single crystals of the K^+ dimer suitable for X-ray diffraction analysis were obtained by diffusion of *n*-hexane to a chloroform solution of the dimer through a dichloromethane buffer solution. The structure of the complex was found to be almost superimposable to that of the Na^+ dimer (Fig. 3 and Fig. S33, ESI†). One K^+ atom is connecting two helices of the same handedness, and another metal ion sits outside the coaxial dimer and fulfils the charge balance of the complex (Fig. S31, ESI†). Q_8-H also afforded the Q_8-Li-Q_8 complex with LiOH, whereas forming Ag^+ or Hg^{2+} dimeric complexes proceeded with acetate salts (Fig. S12–S18, ESI†). ^{1}H NMR spectra of each metal complex presented subtle but significant differences (Fig. 2) depending on the nature of the metal used, indicating that the metal has an influence on the chemical environment of the protons of the dimeric structures. Unlike other metals, the ^{1}H NMR spectrum of the Hg^{2+} complex showed twice as many signals as the other complexes indicating a loss of symmetry (Fig. 2f). This puzzling phenomenon could be explained by close inspection of the solid-state data of the complex (Fig. 3c). While the X-ray structure indicates that the helices backbones of Q_8-Hg-Q_8 are arranged in the same manner as for the Na^+ and K^+ complexes, the Hg^{2+} cation is not positioned at the same position as with alkaline metals. Instead it is closer to one of the two helices rendering the dimer complex dissymmetric. Furthermore, the ^{1}H NMR spectrum of Q_8-Hg-Q_8 shows a set of minor amide proton signals above 11 ppm (Fig. 2f and Fig. S16 and S17, ESI†). These signals do not match those of Q_8-H and likely belong to a Q_8-Hg^+ monomeric species.

Competition experiments were performed by mixing a solution of Q_8-H with equimolar amounts of two metal salts. They revealed the following relative stabilities of the Q_8-M-Q_8 complexes and highlighted the prevalence of Q_8-Ag-Q_8: $K_{Ag} > K_{Na} \approx K_K > K_{Li}$ (Fig. S19–S21, ESI†). The mercury salt was not tested because of its more complicated signal pattern.

The dynamics and possible ligand exchange in the dimeric complexes were investigated by adding a shorter quinoline hexamer, Q_6-H, to a preformed Q_8-Na-Q_8 dimer solution in the presence of excess NaOH. The ^{1}H NMR spectrum of the mixture revealed the formation of the expected symmetric Q_6-Na-Q_6 homodimer and the dissymmetric Q_8-Na-Q_6 heterodimer (Fig. S23–S25, ESI†). The rapid formation of the heterodimer indicates that the metal–ligand bond in the initial Q_8-Na-Q_8 dimer is kinetically labile. This insight led to the investigation of the stereoselectivity of the assembly observed in the crystal and presumed to also exist in solution (*i.e* only helices of similar handedness can form dimers). For this purpose, quinoline oligomers of 8 and 6 units bearing a chiral camphanic group of different chirality at the N-terminus were prepared to yield *R*-Q_8-H and *S*-Q_6-H. This chiral group is known to bias quantitatively the helical handedness of quinoline foldamers in favour of *P* and *M* helices for *R*- and *S*-camphanic groups, respectively.[27] Similarly to the non-chiral analogues, ^{1}H NMR spectra of these individual oligomers in the presence of NaOH indicated the formation of one dimer as a new set of peaks was observed in the ^{1}H NMR spectra. However, when a mixture of *R*-Q_8-H and *S*-Q_6-H was exposed to NaOH, only *S*-Q_6-Na-*S*-Q_6 and *R*-Q_8-Na-*R*-Q_8 homodimers were observed and no *S*-Q_6-Na-*R*-Q_8 heterodimer was detected. The heterodimer formation is prevented by the opposite handedness of *R*-Q_8 and *S*-Q_6. This result demonstrates the chiral narcissistic self-sorting ability of this assembly for which only two helices of identical handedness can coordinate the same metal ion (Fig. S27 and S28, ESI†).

The strong carboxylate-induced complexation led to the proposal that a symmetric foldamer functionalized with carboxylic acid groups at both ends could form either dynamic polymers or macrocyclic structures upon treatment with NaOH or AcOAg. Such a symmetric foldamer, HQ_2PQ_2H (Fig. 4a), containing a central pyridine dicarbonyl unit flanked by two quinolines on each side was prepared. The introduction of hexyl and decyl side chains on the quinoline and pyridine units was crucial for solubility in non polar solvents. After treatment of a chloroform solution of HQ_2PQ_2H with NaOH, the ^{1}H NMR spectrum showed extensive line broadening attributed to the formation of a statistical mixture of oligomers or polymers of variable length (Fig. S35, ESI†). To exert better control over the degree of polymerization, stoppers (*i.e.* monoacids) were introduced to cap the polymer chains and impose a stoichiometric control over the average polymer length. The titration of Q_8-Na-Q_8 with increasing amounts of HQ_2PQ_2H in the presence of NaOH was followed by ^{1}H NMR. After the addition of 1 eq. of the diacid, new sets of peaks were observed (Fig. S36, ESI†). These were attributed to the insertion of one or more diacids to form new oligomeric complexes composed of Q_8 oligomers at each end and one or more HQ_2PQ_2H units in the core, each connected by Na^+ ions. As expected, the amide proton signals of the longer species were shifted upfield. The formation of a statistical mixture of oligomers of various lengths is reflected by the complexity and the number of news signals observed even after the addition of 0.5 equivalents. With the further addition of HQ_2PQ_2H, the signals of the initial Q_8-Na-Q_8 dimer decreased, indicating that Q_8 acted as a stopper in the formation of longer structures.

Circular dichroism (CD) was then applied to probe the elongation of the polymer chains upon insertion of the diacids.

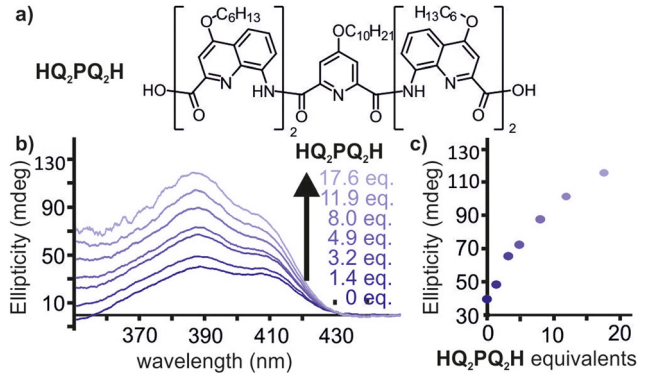

Fig. 4 (b) CD spectra of the titration of a dry $CHCl_3$ solution of R-Q_8H (1 mM, path length 0.1 mm) with increasing amounts of HQ_2PQ_2H in the presence of AcOAg in excess. (c) Plot of the CD intensity at 390 nm depending on the number of equivalents of Q_2PQ_2 added.

The chiral *R*-Q_8-H octamer was used as stopper to dictate the selective assembly of helices of similar handedness. The *P*/*M* equilibrium of the free HQ_2PQ_2H is fast and was expected to shift in favor of *P*-helicity upon insertion in coordinated polymer chains capped with *R*-Q_8. The *P*-helix selective incorporation of HQ_2PQ_2H in coordinated helical chains was evidenced by the amplification of the CD signal as increasing amounts of the racemic diacid was added. Thus, HQ_2PQ_2H was added to a 1 mM solution of *R*-Q_8-H in the presence of an excess of silver acetate, the best mediator for self-assembly. Such a high concentration of stoppers was used to ensure a strong complexation. Increasing amounts of non-chiral diacid produced a continuous increase of the CD signal after equilibration (Fig. 4b and c). Due to the high initial concentration, the CD signal was saturated after the addition of *ca.* 17 equivalents of diacid. The length of the polymer could be estimated from the intensity of the CD signal, which is proportional to the number of quinolines in the oligomer. Assuming that the initial CD signal was due to the 16 quinolines of the initial dimer, the 2.2-fold increase in CD signal indicated that addition of 8 equivalents of diacid generated polymers with 35 quinolines on average, corresponding to the insertion of 4.8 diacids. This metallopolymer represents a foldamer of considerable length that would be difficult to obtain by traditional synthetic methods.

In conclusion, this work describes a novel coaxial ligation of helical foldamers upon metal coordination. Two helical strands possessing one acid termini each were bound by a cation in a head-to-head fashion. The metal coordination transferred the handedness of one foldamer to the other. The use of a bis-acid functionalized foldamer resulted in the formation of supramolecular metallopolymers that were characterized by CD and NMR. The stability of these complexes in organic solvents, the variety of metals that can be used in the assembly, the dynamics of the ligand exchange and the stereoselectivity of the process make this carboxylate-induced ligation of aromatic foldamers a powerful method to create long rods that can find uses in the context of water channeling[12,13] or charge transport properties.[7] Further studies on the rigidity of these supramolecular polymers and their thermodynamic stability are in progress and will be reported in due course.

Conflicts of interest

There are no conflicts to declare.

Notes and references

1 S. H. Gellman, *Acc. Chem. Res.*, 1998, **31**, 173.
2 S. Hecht and I. Huc, *Foldamers: Structure, Properties and Applications*, 2007.
3 V. Corvaglia, I. A. M. Amar, V. Garambois, S. Letast, A. Garcin, C. Gongora, M. D. Rio, C. D-Sabourin, N. Joubert, I. Huc and P. Pourquier, *Pharmaceuticals*, 2021, **14**, 624.
4 C. Tsiamantas, S. Kwon, C. Douat, I. Huc and H. Suga, *Chem. Commun.*, 2019, **55**, 7366.
5 M. Vallade, M. Jewginski, L. Fischer, J. Buratto, K. Bathany, J.-M. Schmitter, M. Stupfel, F. Godde, C. D. Mackereth and I. Huc, *Bioconjugate Chem.*, 2019, **30**, 54.
6 X. Li, N. Markandeya, G. Jonusauskas, N. D. McClenaghan, V. Maurizot, S. A. Denisov and I. Huc, *J. Am. Chem. Soc.*, 2016, **138**, 13568.
7 A. Mendez-Ardoy, N. Markendeya, X. Li, Y.-T. Tsai, G. Pecastaings, T. Buffeteau, V. Maurizot, L. Muccioli, F. Castet, I. Huc and D. M. Bassani, *Chem. Sci.*, 2017, **8**, 7251.
8 S. I. Stupp and L. C. Palmern, *Chem. Mater.*, 2014, **26**(1), 507.
9 C. Tsiamantas, X. de Hatten, C. Douat, B. Kauffmann, V. Maurizot, H. Ihara, M. Takafuji, N. Metzler-Nolte and I. Huc, *Angew. Chem., Int. Ed.*, 2016, **55**, 6848.
10 S. De, B. Chi, T. Granier, T. Qi, V. Maurizot and I. Huc, *Nat. Chem.*, 2018, **10**, 51.
11 X. Yan, P. Weng, D. Shi and Y.-B. Jiang, *Chem. Commun.*, 2021, **57**, 12562.
12 Y. Huo and H. Zeng, *Acc. Chem. Res.*, 2016, **49**, 922.
13 J. Shen, R. Ye, A. Romanies, A. Roy, F. Chen, C. L. Ren, Z. Liu and H. Zeng, *J. Am. Chem. Soc.*, 2020, **142**, 10050.
14 Y. Dai, T. J. Katz and D. A. Nichols, *Angew. Chem., Int. Ed. Engl.*, 1996, **35**, 2109.
15 J. L. Greenfield, F. J. Rizzuto, I. Goldberga and J. R. Nitschke, *Angew. Chem., Int. Ed.*, 2017, **56**, 7541.
16 C. Nuckolls, T. J. Katz, G. Katz, P. J. Collings and L. Castellanos, *J. Am. Chem. Soc.*, 1999, **121**, 79.
17 H. Ito, M. Ikeda, T. Hasegawa, Y. Furusho and E. Yashima, *J. Am. Chem. Soc.*, 2011, **133**(10), 3419–3432.
18 D. Bindl, P. K. Mandal, L. Allmendinger and I. Huc, *Angew. Chem., Int. Ed.*, 2022, **61**, e202116509.
19 L. A. Cuccia, E. Ruiz, J.-M. Lehn, J.-C. Homo and M. Schmutz, *Chem. – Eur. J.*, 2002, **8**, 3448.
20 W. Cai, G.-T. Wang, P. Du, R.-X. Wang, X.-K. Jiang and Z.-T. Li, *J. Am. Chem. Soc.*, 2008, **130**, 13450.
21 T. Qi, T. Deschrijver and I. Huc, *Nat. Protoc.*, 2013, **8**, 693.
22 N. Ahmad, A. H. Chughtai, H. A. Younus and F. Verpoort, *Coord. Chem. Rev.*, 2014, **280**, 1.
23 G. E. Decker, G. R. Lorzing, M. M. Deegan and E. D. Bloch, *J. Mater. Chem. A*, 2020, **8**, 4217.
24 M. Eddaoudi, J. Kim, N. Rosi, D. Vodak, J. Wachter, M. O'Keeffe and O. M. Yaghi, *Science*, 2002, **295**, 469.
25 N. Delsuc, T. Kawanami, J. Lefeuvre, A. Shundo, H. Ihara, M. Takafuji and I. Huc, *Chem. Phys. Chem.*, 2008, **9**, 1882.
26 J. Wang, H. Little, J. Duhamel, X. Li, N. Markandeya, V. Maurizot and I. Huc, *Macromolecules*, 2019, **52**(15), 5829.
27 A. M. Kendhale, L. Poniman, Z. Dong, K. Laxmi-Reddy, B. Kauffmann, Y. Ferrand and I. Huc, *J. Org. Chem.*, 2011, **76**, 195.

